Novel Die Design Using Polytetrafluoroethylene and Polyoxymethylene Creasing Rules for Industrial Die Cutting and Creasing of Dispersion-Coated Folding Boxboards

Roman Lev,[a,*] Johanna Lyytikäinen,[a] Rajesh Koppolu,[b] Panu Tanninen,[a] and Ville Leminen,[a]

*Corresponding author: Roman.Lev@lut.fi

DOI: 10.15376/biores.21.4.18053-10866

GRAPHICAL ABSTRACT

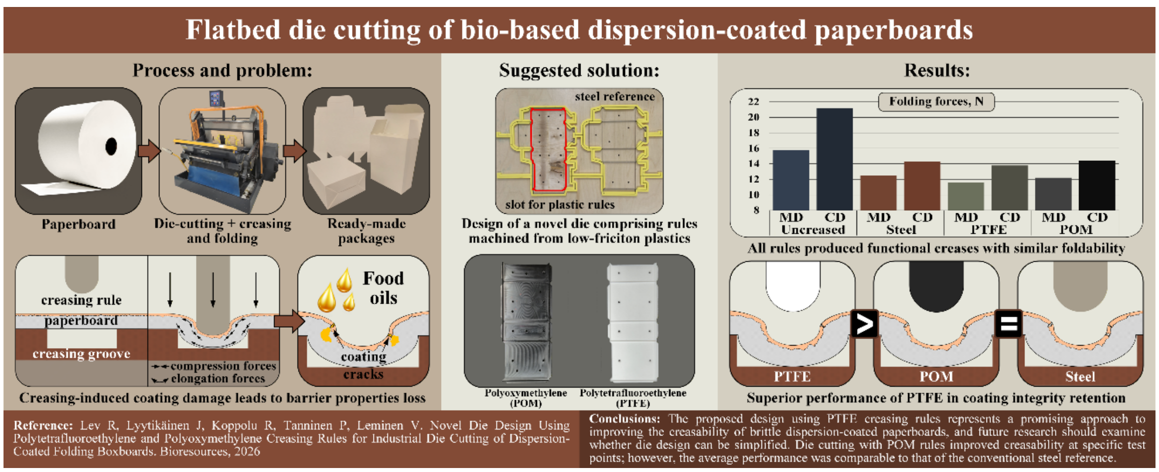

Novel Die Design Using Polytetrafluoroethylene and Polyoxymethylene Creasing Rules for Industrial Die Cutting and Creasing of Dispersion-Coated Folding Boxboards

Roman Lev,[a,*] Johanna Lyytikäinen,[a] Rajesh Koppolu,[b] Panu Tanninen,[a] and Ville Leminen,[a]

The flatbed die-cutting principles used to convert sustainable dispersion-coated paperboards for food packaging have remained largely unchanged for decades, despite persistent issues with coated-surface integrity after creasing. To improve the convertibility of such materials, this study developed novel die incorporating low-friction plastic creasing rules for industrial die cutters. The die comprised conventional uncoated steel creasing rules as the control condition and interchangeable creasing-rule inserts machined from polytetrafluoroethylene (PTFE) or polyoxy-methylene (POM). The rule contours were surrounded by conventional steel knives to produce standard folding-carton blanks from three dispersion-coated paperboards. The coated surface integrity of the materials was evaluated by measuring the oil and grease resistance (OGR) and performing scanning electron microscopy before and after conversion. The results indicated that the highest OGR was obtained for two paperboards creased with PTFE rules. Die cutting with POM rules improved creasability at specific test points; however, the average performance was comparable to that of steel rules. The third paperboard was particularly prone to damage, precluding a comparison across rules. As the PTFE-based toolset demonstrated superior performance on an industrial die cutter, future research should examine whether die design can be simplified by applying a low-friction PTFE coating to conventional steel creasing rules.

DOI: 10.15376/biores.21.4.18053-10866

Keywords: Coated paperboard; Dispersion barrier coatings; Creasability; Foldability; Die cutting; Polytetrafluoroethylene (PTFE); Polyoxymethylene (POM)

*Contact information: a: Mechanical Engineering, Lappeenranta-Lahti University of Technology LUT, Lappeenranta 53850, Finland; b: Biomaterial Processing and Products, VTT Technical Research Center of Finland Ltd., Espoo 02150, Finland; *Corresponding author: Roman.Lev@lut.fi*

INTRODUCTION

Modern coated fibre-based packaging is gradually evolving towards more sustainable solutions, prioritising the recyclability and biodegradability of packaging materials. Accordingly, substantial research has focused on developing new substrates and coatings to meet sustainability targets. Conversely, the core technologies underpinning flatbed die cutting of coated paperboards have remained unchanged for decades. Although conventional plastic coatings typically exhibit sufficient elasticity to withstand the die-cutting process (Leminen *et al.* 2018; Tanninen *et al.* 2015a,b), novel dispersion-coated materials may crack under an applied load (Tanninen *et al.* 2014, 2015b). Therefore, traditional die-cutting tools require adaptation to improve the creasability of dispersion-coated substrates.

Die cutting—typically categorised as flatbed or rotary—is the most common method for blank preparation in packaging production, owing to high automation and throughput (Bota *et al.* 2022; Kirwan 2013). A flatbed die is a wooden form that incorporates laser-cut channels with cutting knives and creasing rules, which are traditionally manufactured from thin metal strips. The knives are usually surrounded by a compressible material that holds the paperboard during cutting. In the flatbed die-cutting machine used in this study (Fig. 1a), the die was mounted on a stationary steel plate, whereas the counterpart (matrix) was mounted on a moving plate. A paperboard sheet was inserted when the platen was open. During the cutting cycle, the platen closed and the knives cut the material *via* 'kiss' contact against a backing steel plate; simultaneously, the rounded-edge creasing rules pressed the paperboard into grooves cut in the matrix (Kirwan 2013; Tanninen *et al.* 2015b). Flatbed die cutting is typically preferred for short-to-medium production runs, where higher precision and lower tooling costs are advantageous.

Flatbed die cutters operate using a 'crush' cutting method, in which knives are driven vertically through the paperboard. Producing all cuts and creases simultaneously in a single machine stroke at high speeds (up to 100 blanks/min) requires substantial pressing force (Kirwan 2013; Leminen *et al.* 2019). Compared with other creasing methods, flatbed die cutting can produce deeper creases with a more defined geometry and improved foldability (Leminen *et al.* 2019, 2021). However, during this process, the paperboard is exposed predominantly to compressive loading, which can induce pinholes and cracks in the dispersion-coated layer (Kuusipalo 2001; Tanninen *et al.* 2015b). Although reducing the die-cutting force may mitigate surface damage, it can also compromise crease functionality (Marin *et al.* 2022; Tanninen *et al.* 2015b). An alternative approach is to reduce friction between the paperboard and the creasing rules, thereby lowering process intensity (Tanninen *et al.* 2015b; Vishtal *et al.* 2014).

In the previous study, it was reported that the friction between creasing tools and paperboard can be reduced by replacing steel creasing rules with machinable plastics such as polytetrafluoroethylene (PTFE) and polyoxymethylene (POM) (Lev *et al.* 2026). At laboratory scale, these plastic rules improved performance by preserving crease functionality while minimising surface damage to the dispersion coating. However, industrial machinery exposes paperboard structures to considerably higher stresses, underscoring the need to assess the effectiveness of plastic rules under harsher conditions.

To address this gap, this study investigated the performance of a novel die incorporating plastic creasing rules during the industrial production of folding carton blanks. Performance was evaluated by measuring oil and grease resistance (OGR) before and after converting the paperboards using plastic and conventional creasing rules, and by comparing the extent of induced surface damage. Scanning electron microscopy (SEM) was performed to correlate the surface damage with the barrier properties.

MATERIALS AND METHODS

Materials

Three dispersion-coated paperboards were examined in this study (Table 1). These materials represent more sustainable alternatives to conventional plastic-coated boards and may benefit from modified creasing-rule materials. Thickness and grammage were determined in accordance with ISO 534 and ISO 536, respectively. The first material was a commercial dispersion-coated paperboard, MetsäBoard Prime FBB EB (Metsä Board Oyj, Finland), hereafter referred to as EB. The second material was a MetsäBoard Prime FBB Bright substrate (MetsäBoard, Finland) coated with a commercial dispersion, CHP BAR D. This dispersion comprised binders and pigments and was supplied as an industrial reference sample by CH Polymers Ltd. (Finland). The third material used the same substrate with a double-layer coating of CHP BAR D. The latter two paperboards are referred to as test points 1 and 2 (TP1 and TP2), respectively, reflecting the number of coated barrier layers. TP1 and TP2 were produced on the SUTCO pilot coating line at VTT (VTT Bioruukki, Espoo, Finland) using a reverse gravure coating method at a speed of 20 m/min. The gravure roll had a volume of 75 cc/m^2 and a mesh size of 20 lines/cm. The coating dispersion had a solids content of 50%. Despite differences in grammage (Table 1), TP1 and TP2 exhibited similar mean thicknesses, likely due to the substantial thickness variation in the base substrate reported by the manufacturer (± 4%). After coating, the TP1 and TP2 rolls were cut into 50 cm × 50 cm sheets. All materials were stored under standard conditions (23 °C, 50% relative humidity) for at least 24 h prior to testing.

Table 1. Material Properties

Code	Coating name	Total material grammage (gsm)	Total material thickness (µm)	Coating thickness (µm)
EB	EB	226 ± 9	346 ± 14	17 ± 9 (Lev *et al.* 2024)
Unc-PB	Uncoated substrate for TP1 and TP2	210 ± 4	300 ± 9	—
TP1	CHP BAR D, 1 layer	219 ± 1	316 ± 1	16 ± 1
TP2	CHP BAR D, 2 layers	224 ± 2	316 ± 2	16 ± 2

Tooling Design

A die for the cutting machine was produced by Finn-Fold Oy (Vantaa, Finland) using manufacturing drawings prepared by LUT Packaging Technology. The die combined conventional steel and novel plastic creasing rules within a single tool, requiring two cutting contours on the form (Fig. 1c). The overall dimensions of the two contours on the die were 491 mm × 316 mm. The right-hand contour comprised typical steel creasing rules and cutting knives, surrounded by a compressible material to retain the blank during the cutting cycle. The left-hand contour used the same configuration of steel knives; however, the region intended for creasing rules incorporated a slot milled into the plywood.

A slot with a complex geometry was designed to accommodate inserts manufactured from PTFE and POM (Fig. 1d). The inserts were machined with a contour corresponding to the steel creasing rules used on the right-hand side of the die. Additional material was incorporated around the plastic creasing rules to reinforce the inserts and prevent bending under load. Three steel creasing rules were retained within the contour to simplify the insert design. The contours produced standard folding-carton blanks, as shown in Fig. 1e, which were folded into cartons with dimensions 100 mm × 50 mm × 120 mm (Fig. 1f). All parameters for the creasing rules and matrices were defined and justified in a previous study (Lev *et al.* 2026); accordingly, all creasing rules had a round-tip profile with a facet radius of 0.36 mm, a width of 2 pt (0.71 mm) and a height of 3 mm. The gap between the plastic rules and steel knives was set to approximately 0.5 mm, matching the nominal spacing between the steel rules and knives in the right-hand contour. Although the cross direction (CD) typically requires deeper creasing, industrial tools are manufactured with uniform rule heights; therefore, the plastic rules were machined to the same height to minimise variations in the creasing process between plastic and steel tools.

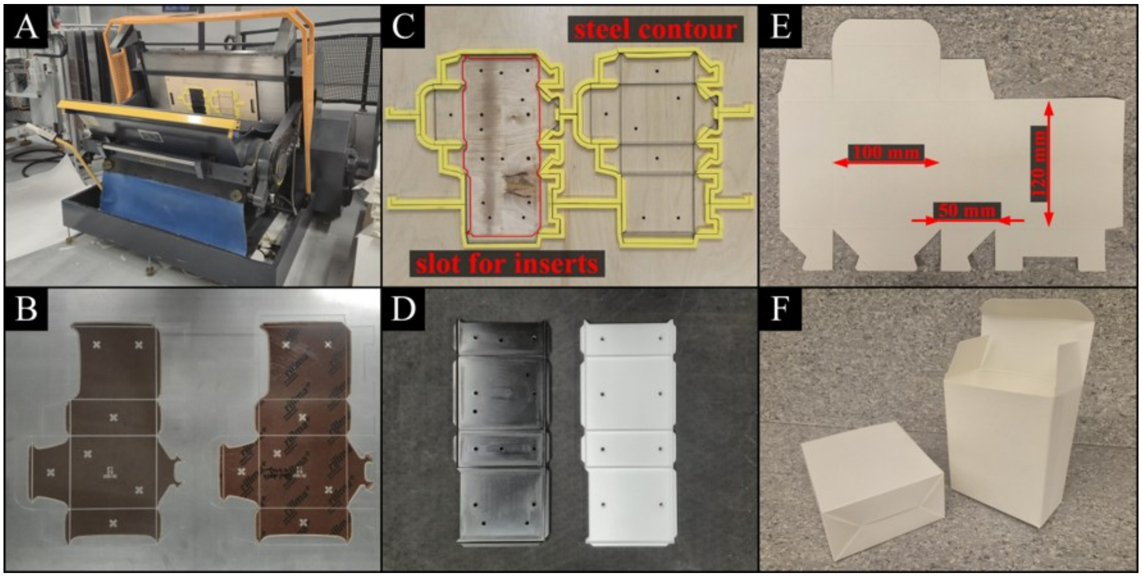

Fig. 1. Cutting and creasing tools: (a) an industrial die cutter with installed tools; (b) a lower metal plate with matrices; (c) a die with two cutting and creasing contours; (d) POM (black) and PTFE (white) inserts; (e) a flat carton blank produced with the die; and (f) ready-made cartons folded from the blanks

Material-Creasing Rule Coefficient of Friction

The kinetic coefficients of friction between the paperboards and the rule materials were measured in accordance with ASTM D 1894–01. Procedural modifications for plastic tools were described in a previous study (Lev *et al.* 2026). For each paperboard, six specimens per fibre direction were tested (Table 2). Across all paperboards, PTFE yielded the lowest coefficient of friction, followed by POM and then steel.

Table 2. Kinetic Coefficients of Friction Between the Paperboards and Creasing Rule Materials

Paperboard	Rule Material					
	Steel		PTFE		POM	
	MD	CD	MD	CD	MD	CD
EB	0.268	0.245	0.159	0.165	0.176	0.197
TP1	0.294	0.289	0.135	0.125	0.147	0.142
TP2	0.267	0.260	0.135	0.124	0.144	0.139

Die Cutting and Creasing

The industrial die cutter used in this study was a Ruiyang ML1200 (Wenzhou, Zhejiang, China) (Fig. 1a). The machine allowed only adjustment of the gap between the plates at the end of the cutting cycle; this setting was used to produce creases of different depths. Initially, the materials were creased to a groove depth of 100 μm to enable comparison of different creasing rules under harsher conditions. However, OGR measurements revealed excessive surface damage in TP1 and TP2 following creasing parallel to the machine direction (MD), and the target depth was therefore reduced to 60 μm for both materials. This depth was considered optimal for achieving adequate crease formation while minimising surface damage (Lev *et al.* 2025, 2026; Marin *et al.* 2022; Tanninen *et al.* 2021). Considering paperboard anisotropy (Kim *et al.* 2010), blanks with the most uniform MD and CD crease depths were obtained when the longer side of the carton was oriented parallel to the MD. Two sets of matrices were used: for creasing TP1 and TP2 to 60 μm, the matrix groove depth was 430 μm, whereas for creasing EB to 100 μm, a depth of 590 μm was used (Fig. 1c). All matrix grooves were 1.5 mm wide. Crease depths were measured using a Keyence VR 3200 optical 3D profilometer (Keyence, Itasca, USA).

Folding

To ensure comparable functionality of creases produced using steel and plastic rules, creases were folded using a folding test setup mounted on a Shimadzu AGS-X material tester (Shimadzu, Kyoto, Japan). A detailed description of this folding arrangement is provided by Lev *et al.* (2026). Folding specimens were cut from the carton blanks, and the crease length in each specimen was 65 mm. Each specimen was clamped approximately 1 mm from the centre of the crease, and a folding rule was positioned approximately 2 mm from the clamps, resulting in a folding angle of approximately 89°. Folding was performed at the maximum crosshead speed of the material tester (1000 mm/min), corresponding to an angular folding speed of approximately 74.2°/s. At least five samples for each fibre direction were folded towards the bead, with the specimens clamped such that the coated side faced upwards. All folded specimens were subsequently tested for OGR.

OGR Measurements

Oil and grease resistance was tested according to ISO 16532-1. First, all materials were tested in the unconverted state to establish a baseline for comparison with the converted samples. The OGR of the converted materials was then evaluated at several test points using combinations of the following variables: (1) creasing rule material (steel, PTFE, or POM), (2) creasing direction (parallel to the MD or CD), and (3) folding condition (unfolded or folded). During the tests with converted materials, an oil drop and a 50-g weight with a diameter of 3 cm were applied exactly in the middle of the creased/folded line of each sample to maximise the utilisation of the converted area. At each test point, at least five replicate specimens were tested in parallel, placed in an oven at 40 °C. In line with the previous study, failure time was recorded only when oil penetration occurred within the creased area, to focus on the effects of creasing rule material on the integrity of the dispersion coatings (Lev *et al.* 2026).

SEM imaging

Samples were sputter-coated with gold using an Edwards Scancoat Six Sputter Coater, after which SEM imaging was performed using a Hitachi SU3500 microscope (Tokyo, Japan). A secondary electron detector was used with an accelerating voltage of 5 kV, and the working distance was maintained at approximately 5 mm for all samples.

RESULTS AND DISCUSSION

Die Cutting and Creasing

The average depths of the produced creases ± standard deviations (SD) are presented in Table 3. Achieving the target depths required adjustment of the gap between the die-cutter plates and careful alignment of the creasing rules with the matrix grooves. All MD and CD creases were produced from blanks manufactured using the same die-cutter settings. After sample production, the plastic rules were confirmed to be neither damaged nor bent.

Table 3. Average Depths of the Produced Creases

Paperboard	Creasing Depth ± SD, µm					
	EB		TP1		TP2	
	MD	CD	MD	CD	MD	CD
Steel	104 ± 6	98 ± 7	63 ± 2	65 ± 4	62 ± 4	62 ± 2
PTFE	100 ± 5	96 ± 4	59 ± 4	63 ± 6	64 ± 4	65 ± 4
POM	96 ± 3	99 ± 7	64 ± 3	66 ± 2	63 ± 2	67 ± 3

Folding Results

The forces required to fold the samples are shown in Fig. 2. All creasing rules produced functional creases, with similar folding forces at the corresponding test points and only minor deviations. Figure 2 shows the typical anisotropic behaviour observed for EB and TP2. When the uncreased materials required considerably higher folding forces than the creased samples, the folding resistance along MD was consistently lower than that parallel to CD. Although uncreased TP1 also exhibited reduced foldability, the expected trend between fibre directions was not observed. The single-coated TP1 presumably behaved in a more substrate-dominated manner, where local damage and deformation mechanisms may have masked the directional differences.

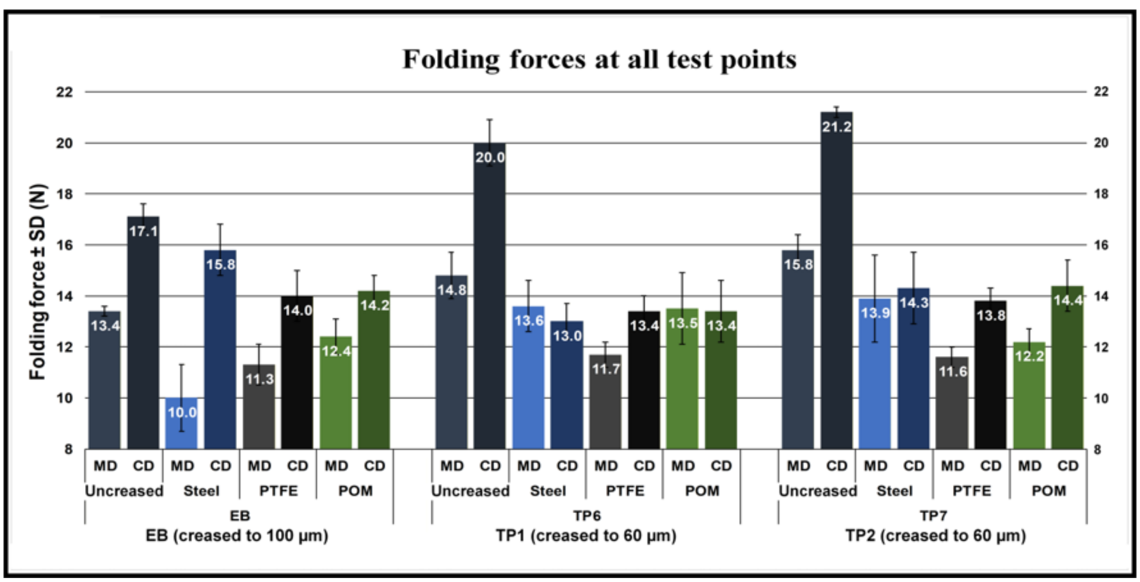

Fig. 2. Forces required to fold the material samples at all test points

OGR Results

The OGR test results are presented for each material and test point. The numbers at the top and bottom of each bar represent the minimum and maximum oil penetration times, respectively. Where applicable, the bar centre denotes the mean value, calculated and reported in accordance with the OGR standard applied in this study. Mean values could not be calculated for test points with an OGR of 6–24 h or 24+ h because these categories do not provide discrete penetration times. The graph axes were scaled to emphasise differences among lower-OGR test points; consequently, failure times exceeding 6 h are not scaled appropriately. Folding performance was clearly influenced by the preceding creasing procedure; however, coating damage may also arise from mechanisms unrelated to creasing, such as rupture of the outer coated layer by substrate fibres during folding (Giampieri *et al.* 2011). Therefore, comparisons between creasing rules are primarily based on the performance of samples that were creased only.

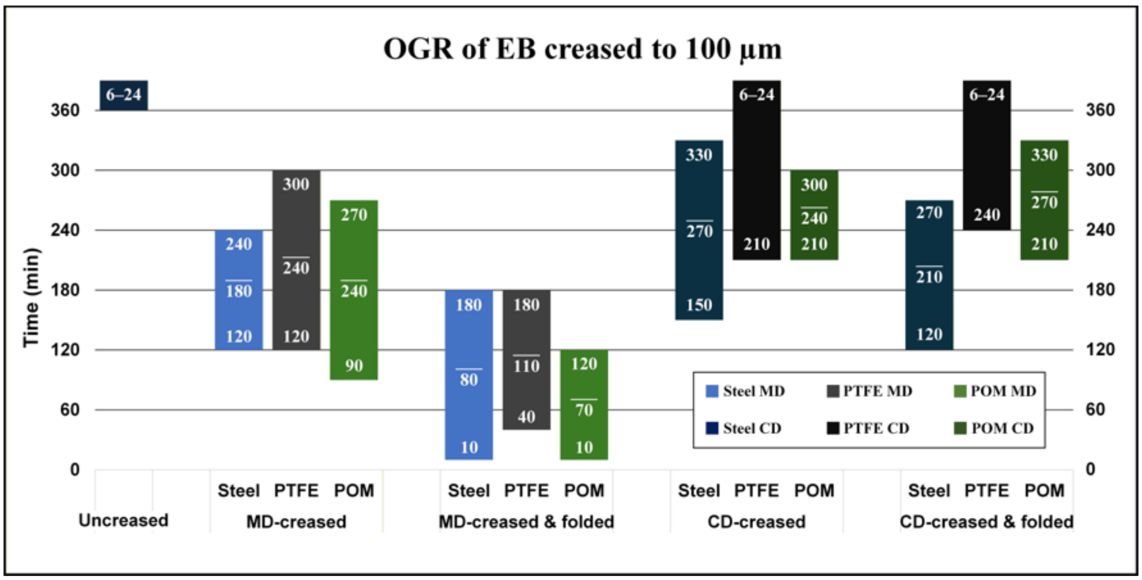

Fig. 3. OGR of EB at different test points

The OGR of EB across test points is shown in Fig. 3. All unconverted samples failed between 6 and 24 h of testing, with oil penetrating the entire tested area. For all rule materials, the MD-creased-and-folded samples exhibited a lower OGR than the corresponding creased-only samples. This trend was not observed for CD creasing with plastic rules, for which folding did not substantially reduce OGR. The PTFE-creased samples generally exhibited longer OGR times than the steel- and POM-creased samples for this material. Following CD creasing and folding with PTFE, some samples performed similarly to the uncreased material. The performance of POM relative to steel was inconsistent, with results varying across test points.

In the previous study (Lev *et al.* 2026), EB was tested at the laboratory scale by using one-rule creasing toolsets manufactured from the same materials (steel, PTFE, and POM). Consistent with the present findings, the steel-creased material generally exhibited a lower OGR than the plastic-creased material; however, several samples achieved OGR values comparable to unconverted paperboard at most test points, irrespective of the creasing method. In this study, apart from the two PTFE-creased test points, all EB samples failed before reaching the initial 6 to 24 h range, highlighting the markedly harsher conversion conditions experienced when using industrial machinery. Possible contributors include the considerably higher cycle speeds (one stroke in less than 0.5 s versus approximately 2 s with laboratory toolsets) and the inclusion of a cutting operation, which increases conversion forces. However, deeper creasing to 100 µm was applied here to enable comparison of creasing rules, although such depth would be unnecessary in commercial packaging production.

The OGR results for TP1 are presented in Fig. 4. In the unconverted state, OGR ranged from 6 to 24 h. After MD creasing with all rule materials, OGR decreased markedly, with a maximum of 90 min. Subsequent folding reduced OGR to several minutes, indicating severe coating damage. Conversely, CD-oriented creasing preserved the initial OGR at all test points, even after folding. This greater susceptibility to damage in MD was attributed to inherent material properties rather than to differences among creasing rules.

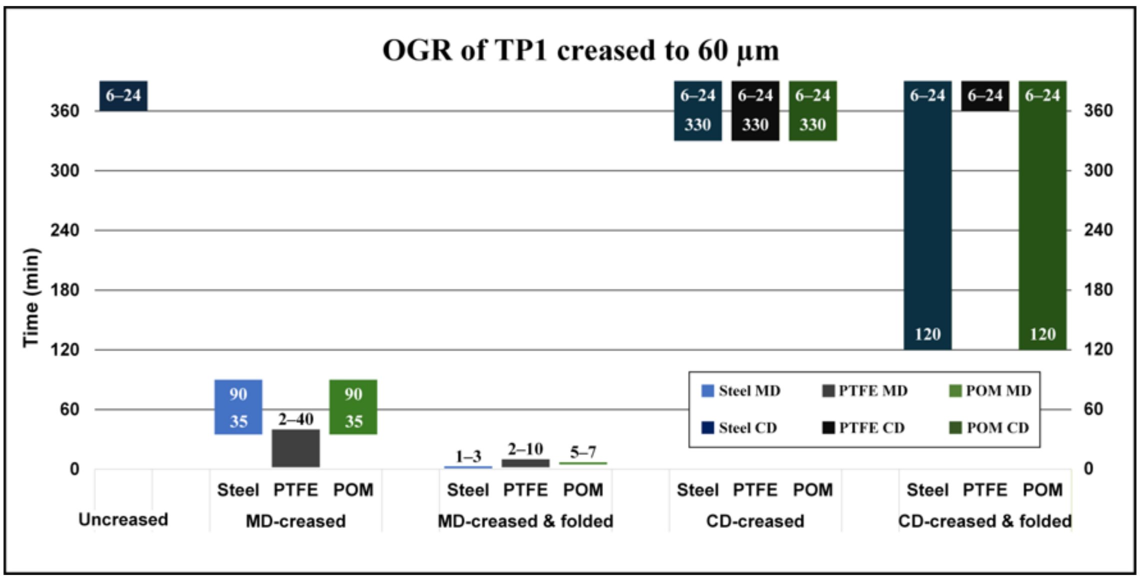

Fig. 4. OGR of TP1 at different test points

The additional coating layer on TP2 substantially enhanced the material properties compared with TP1 (Fig. 5). None of the unconverted samples exhibited back-side oil marks after 24 h. After MD creasing with steel, OGR decreased sharply in several samples; this reduction was less pronounced after creasing with PTFE and was not observed after creasing with POM. However, after creasing with steel or POM, the folded samples performed similarly, and the coating showed severe surface damage. In contrast, several PTFE-creased and folded samples resisted oil for more than 24 h and exhibited the same OGR as the unconverted material. While TP1 performed adequately with a single coating layer after CD creasing and folding, the double-layer coating on TP2 was completely unaffected by conversion with any creasing rule at these test points, and all samples appeared grease-proof.

Overall, the industrially produced EB exhibited a clear improvement in convertibility after creasing with the PTFE rules, particularly after CD creasing. The material was more susceptible to damage when creased parallel to MD; however, the creasability differences between the fibre directions were less pronounced than those observed for the other materials. Unlike the previous study (Lev *et al.* 2026), increasing the stroke length for CD creasing was neither feasible nor required, and both directions were therefore creased using similar parameters within a single die-cutting cycle. This produced higher convertibility along CD, consistent with behaviour typically reported for dispersion-coated paperboards (Lev *et al.* 2024; Nygårds *et al.* 2014). Conversely, the strong directional dependence of TP1 precluded a meaningful comparison of the creasing rules, as all toolsets caused severe damage during MD creasing and substantially less damage during CD creasing. Finally, the PTFE rules demonstrated superior performance for the MD creasing of TP2 as observed for EB; however, rule performance after CD creasing could not be compared because TP2 exhibited markedly high convertibility in this direction.

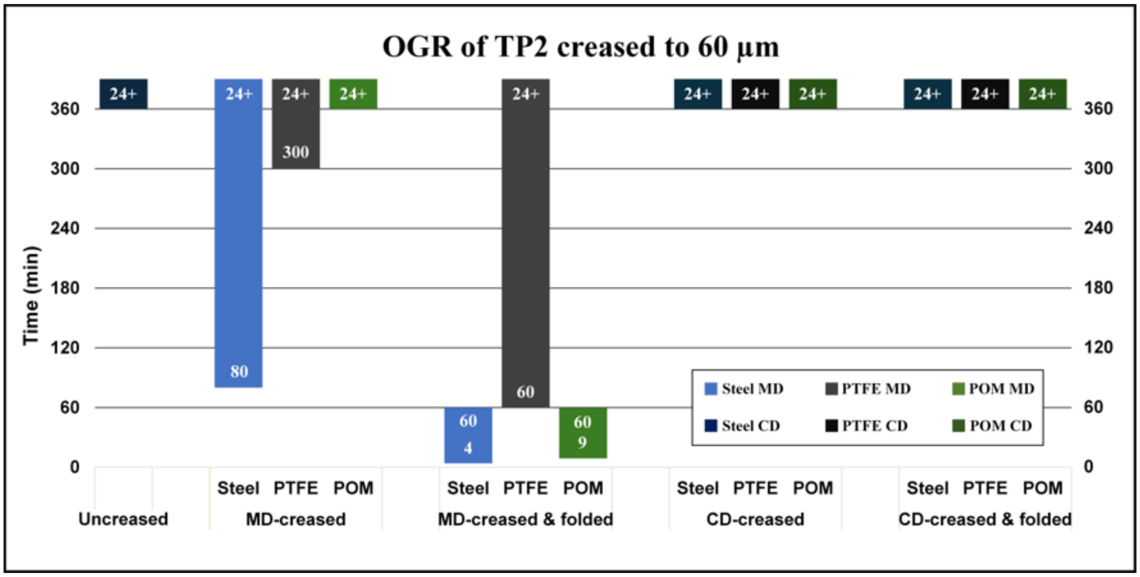

Fig. 5. OGR of TP2 at different test points

SEM Results

Scanning electron microscopy was performed on the material samples at different test points to characterise damage induced on the coated surfaces after creasing and folding. The images are presented in Figs. 6, 7, and 8 for EB, TP1, and TP2, respectively. SEM was performed on the samples converted parallel to the MD because they experienced greater damage than the CD-converted samples. Where applicable, the crease bottoms are highlighted by transparent red regions, and rectangular boxes with red arrows indicate the magnified areas of interest.

The EB surface contained occasional irregularities, the deepest of which may be pinholes that could adversely affect the barrier performance of the material (Fig. 6a, b). In some cases, oil permeated through these pinholes markedly faster than through the creased areas, suggesting that coating-process-related surface defects can be more detrimental than conversion-induced damage. Figure 6c shows the surface with a representative crease produced using the POM rule. The magnified region in Fig. 6d shows surface grazes, likely arising from a minor irregularity on the creasing rule surface and an internal defect resembling a pinhole within the crease. Oil penetration through such pinholes may be misattributed to creasing-induced defects during OGR measurements; however, these events could not be excluded from the dataset. Examples of these creased and folded regions exhibiting deep, conversion-induced cracks are presented in Fig. 6e, f. Such damage can form unrestricted paths for oil permeation, markedly compromising the coating barrier function.

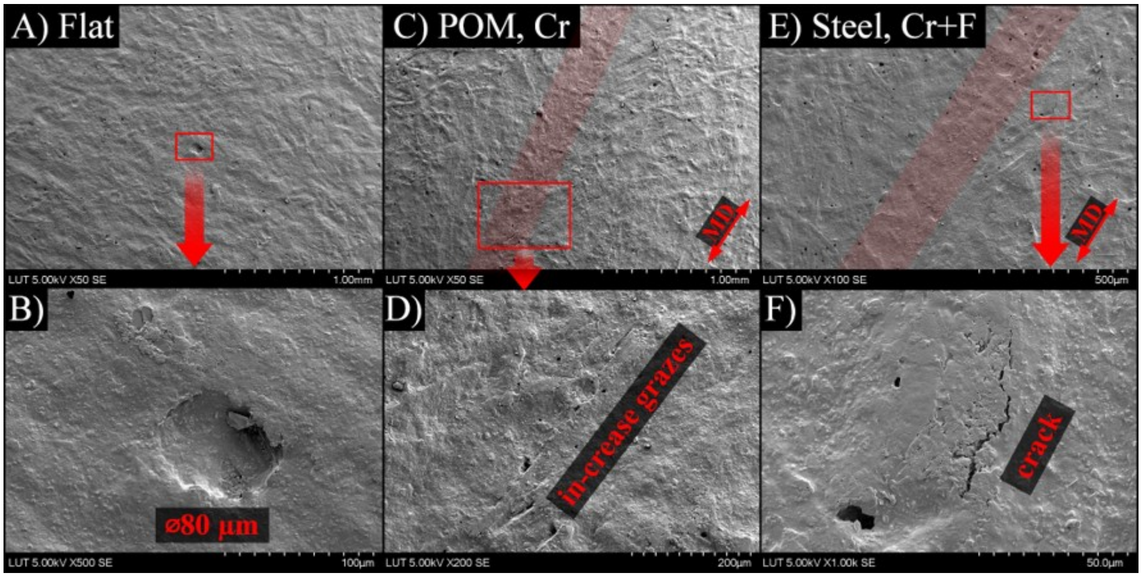

Fig. 6. SEM images of EB. "Flat" – a sample was not converted or exposed to oil; "Cr" – a sample was creased; "Cr+F" – a sample was creased and folded: (a) unconverted reference surface; (b) enlarged area with a surface irregularity; (c) a POM-creased sample; (d) inside-crease grazes; (e); (f) a steel-creased and folded sample with a conversion-induced crack

Figure 7a shows the unconverted surface of TP1, which was rougher than the double-layer-coated surface of flat TP2 (Fig. 8a).

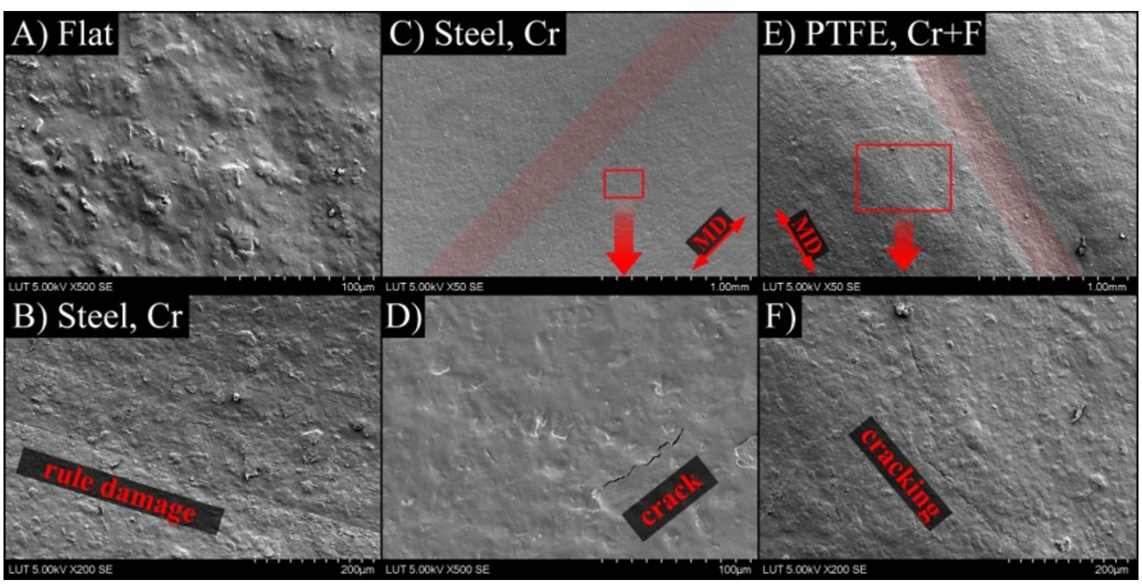

Fig. 7. SEM images of TP1. "Flat" – a sample was not converted or exposed to oil; "Cr" – a sample was creased; "Cr+F" – a sample was creased and folded: (a) unconverted reference surface; (b) damage from steel rule irregularities on the crease bottom; (c), (d) a steel-creased sample with a crack next to the crease bottom; (e), (f) a PTFE-creased and folded sample with multiple conversion-induced cracks

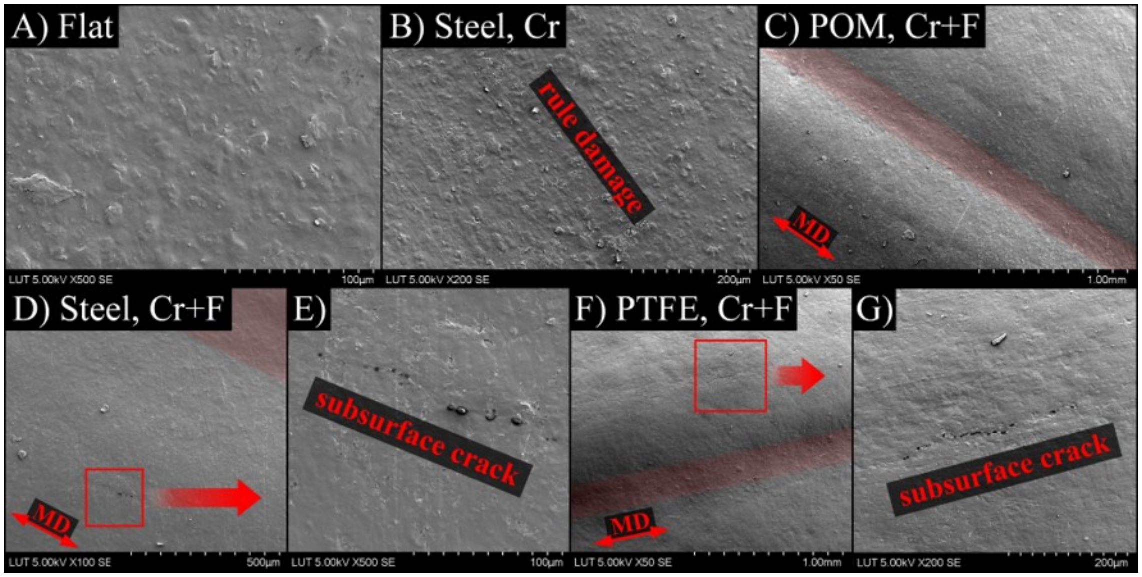

Fig. 8. SEM images of TP2. "Flat" – a sample was not converted or exposed to oil; "Cr" – a sample was creased; "Cr+F" – a sample was creased and folded: (a) unconverted reference surface; (b) damage from steel rule irregularities on the crease bottom; (c) a POM-creased and folded sample without visible damage; (d), (e) a steel-creased and folded sample with a subsurface crack; (f), (g) a PTFE-creased and folded sample with a subsurface crack

In addition to typical creasing defects occurring away from the crease bottom, creasing with steel rules produced inside-crease damage in both TP1 and TP2, which can be attributed to irregularities on the rule surface (Fig. 7b and Fig. 8b, respectively). The damage was more severe in TP1, consistent with the pronounced differences in OGR between the materials. By contrast, such inside-crease damage was not observed after creasing with the plastic rules (*e.g.*, Fig. 8c). A representative creasing-induced crack propagating through the coating layer is shown in Fig. 7c, d. Following folding, the crack density increased substantially, corresponding to a marked reduction in OGR (Fig. 7e, f). In contrast, TP2 exhibited less damage within the coated layers than TP1 (Fig. 8d, f), even after both creasing and folding. Figure 8e, g shows subsurface cracks in the lower dispersion-coated layer, while the top layer exhibited localised oil penetration (dark spots). These cracks may have originated from the substrate and propagated towards the surface, causing a partial loss of coating integrity. Nevertheless, the extent and severity of the damage in TP2 were considerably reduced by the additional coating layer, as confirmed by both OGR measurements and SEM observations.

Study Limitations

This study has several limitations. First, variations in paperboard production quality may cause thickness non-uniformity; this should be addressed by testing a sufficient number of samples at each test point to minimise the influence of such variability. Second, pre-existing surface defects (*e.g.*, pinholes) may be present in the creased areas; oil penetration through these features could therefore be misinterpreted as penetration through creasing-induced defects. Third, manual adjustment of the creasing rules and matrix grooves may introduce minor misalignment between their centre lines. Fourth, folding tests were constrained by the maximum speed of the material tester, which prevented folding at industrial line speeds.

Implications and Future Work

Overall, PTFE creasing rules provided a moderate improvement in the convertibility of the investigated materials, and the proposed approach represents a practical route to improving the creasability of brittle dispersion-coated paperboards in industrial die cutting. Given that PTFE-based creasing toolsets were effective at both laboratory and industrial scales, future work should focus on simplified tool designs that combine the durability of steel rules with a low-friction PTFE coating.

CONCLUSIONS

1. A novel die for an industrial die cutter was successfully developed in this study. The die was designed to incorporate low-friction plastic creasing rules machined from polytetrafluoroethyelene (PTFE) and polyoxymethylene (POM). The test results showed generally higher oil and grease resistance (OGR) values for materials creased with PTFE rules than for conventional steel rules at multiple test points.
2. Folding tests confirmed that all creasing rules produced functional creases requiring considerably lower folding forces than the unconverted materials, with only minor deviations between corresponding test points.
3. Although the POM rules improved performance at certain test points, their mean performance was comparable to that of the conventional steel rules, underscoring the importance of polymer selection to fully utilise the benefits of the proposed low-friction creasing approach.
4. The surface defects observed by scanning electron microscopy (SEM) at different test points were consistent with the OGR results.

ACKNOWLEDGMENTS

This research was conducted as part of the Coatings and composites from novel biobased dispersions (COCOBIN) project (No. 190/31/2024), partially funded by Business Finland, which is gratefully acknowledged.

Data Availability

The data that support the findings of this study are available from the corresponding authors upon reasonable request.

Conflict of Interest

The authors declare no potential conflicts of interest.

REFERENCES CITED

Bota, J., Pibernik, J., Kovačević, D., and Brozović, M. (2022). "The effects of flatbed creasing tool on printed paperboard," in: *Proceedings - The Eleventh International Symposium GRID 2022*, pp. 657-663, University of Novi Sad, Faculty of Technical Sciences, Department of Graphic Engineering and Design.

Giampieri, A., Perego, U., and Borsari, R. (2011). "A constitutive model for the mechanical response of the folding of creased paperboard." *International Journal of Solids and Structures* 48 (16–17), 2275-2287. https://doi.org/10.1016/j.ijsolstr.2011.04.002

Kim, C.-K., Lim, W.-S. and Lee, Y. K. (2010). "Studies on the fold-ability of coated paperboard (I): Influence of latex on fold-ability during creasing/folding coated paperboard," *Journal of Industrial and Engineering Chemistry* 16(5), 842-847. https://doi.org/10.1016/j.jiec.2010.05.001

Kirwan, M. J. (2013). *Handbook of Paper and Paperboard Packaging Technology*. 2nd Ed., John Wiley & Sons, Incorporated, Chichester, West Sussex, UK.

Kuusipalo, J. (2001). "Starch-based polymers in extrusion coating," *Journal of Polymers and the Environment* 9(3), 125-135.

Leminen, V., Matthews, S., Tanninen, P., and Varis, J. (2018). "Effect of creasing tool dimensions on the quality of press-formed paperboard trays." *Procedia Manufacturing* 25, 397-403. https://doi.org/10.1016/j.promfg.2018.06.109

Leminen, V., Tanninen, P., Matthews, S., Pesonen, A., and J. Varis, J. (2019). "The effect of creasing method and tooling on the geometry of formed creases in the creasing process of coated and uncoated paperboard," 20014. Vitoria-Gasteiz, Spain.

Leminen, V., Niini, A., Tanninen, P., and Matthews, S. (2021). "Comparison of creasing and scoring in the manufacturing of folding cartons," *Procedia Manufacturing* 55, 221-225. https://doi.org/10.1016/j.promfg.2021.10.031

Lev, R., Lyytikäinen, J., Matthews, S., Koppolu, R., Tanninen, P., and Leminen, V. (2024). "Investigating the convertibility and barrier performance of a novel suberin dispersion coating during the paperboard creasing process." *Packaging Technology and Science* 37(11), 1037-1048. John Wiley and Sons Ltd. https://doi.org/10.1002/pts.2845

Lev, R., Pesonen, A., Lyytikäinen, J., Tanninen, P., and Leminen, V. (2025). "Investigating the performance of polytetrafluoroethylene and polyoxymethylene creasing rules in the package conversion of coated paperboard," *Packaging Technology and Science* 39(8), 1003-1014. https://doi.org/10.1002/pts.70071

Lev, R., Pesonen, A., Lyytikäinen, J., Tanninen, P., and V. Leminen, V. (2026). "Investigating the performance of polytetrafluoroethylene and polyoxymethylene creasing rules in the package conversion of coated paperboard." *Packaging Technology and Science*. https://doi.org/10.1002/pts.70071

Marin, G., Nygårds, M., and Östlund, S. (2022). "Experimental quantification of differences in damage due to in-plane tensile test and bending of paperboard," *Packaging Technology and Science* 35(1), 69-80. https://doi.org/10.1002/pts.2608

Nygårds, M., Bhattacharya, A., and Krishnan, S. (2014). "Optimizing shear strength profiles in paperboard for better crease formation," *Nordic Pulp & Paper Research Journal* 29(3), 510-520. https://doi.org/10.3183/npprj-2014-29-03-p510-520.

Tanninen, P., Lindell, H., Saukkonen, E., and Backfolk, K. (2014). "Thermal and mechanical durability of starch-based dual polymer coatings in the press forming of paperboard." *Packaging Technology and Science* 27(5), 353-363. John Wiley and Sons Ltd. https://doi.org/10.1002/pts.2036

Tanninen, P., Leminen, V., Eskelinen, H., Lindell, H., and Varis, J. (2015a). "Controlling the folding of the blank in paperboard tray press forming," *BioResources* 10(3), 5191-5202. https://doi.org/10.15376/biores.10.3.5191-5202

Tanninen, P., Saukkonen, E., Leminen, V., Lindell, H., and Backfolk, K. (2015b). "Adjusting the die cutting process and tools for biopolymer dispersion coated paperboards," *Nordic Pulp & Paper Research Journal* 30(2), 336-343.

Tanninen, P., Matthews, S., Leminen, V., and Varis, J. (2021). "Analysis of paperboard creasing properties with a novel device," *Procedia Manufacturing* 55, 232-237. https://doi.org/10.1016/j.promfg.2021.10.033

Vishtal, A., Hauptmann, M., Zelm, R., Majschak, J.-P., and Retulainen, E. (2014). "3D forming of paperboard: The influence of paperboard properties on formability," *Packaging Technology and Science* 27(9), 677-691. https://doi.org/10.1002/pts.2056

Article submitted: May 15, 2026; Peer review completed: May 31, 2026; Revised version received and accepted: September 7, 2026; Published: September 18, 2026.
DOI: 10.15376/biores.21.4.10853-10866